Energy Materials

Supplementary Materials

In-situ construction of artificial interface layer using sodiophilic Bi_2S_3 nanowires for dendritic-free sodium-metal batteries

Jiazhe Li[1,2], Jiyi Li[3], Yu Qiao[1,2], Daxian Cao[3], Xin Ji[2], Weijiang Xue[3,4], Guiyin Xu[1,5], Hengda Sun[1,5], Xiaogang Han[2], Hongkang Wang[1,2,*]

[1]Pingdingshan Industrial Technology Research Institute, Henan Academy of Sciences, Zhengzhou 450046, Henan, China.

[2]State Key Lab of Electrical Insulation and Power Equipment, Center of Nanomaterials for Renewable Energy (CNRE), School of Electrical Engineering, Xi'an Jiaotong University, Xi'an 710049, Shannxi, China.

[3]State Key Laboratory of Advanced Papermaking and Paper-Based Materials, Plant Fiber Research Center, School of Light Industry and Engineering, South China University of Technology, Guangzhou 510641, Guangdong, China.

[4]Center for Advancing Materials Performance from the Nanoscale (CAMP-Nano), State Key Laboratory for Mechanical Behavior of Materials, Xi'an Jiaotong University, Xi'an 710049, Shannxi, China.

[5]State Key Laboratory for Modification of Chemical Fibers and Polymer Materials, College of Materials Science and Engineering, Donghua University, Shanghai 201620, China.

[*]**Correspondence to:** Dr. Hongkang Wang, State Key Lab of Electrical Insulation and Power Equipment, Center of Nanomaterials for Renewable Energy (CNRE), School of Electrical Engineering, Xi'an Jiaotong University, Xi'an 710049, Shannxi, China. E-mail: hongkang.wang@mail.xjtu.edu.cn

ORCID: Hongkang Wang (0000-0003-4893-5190)

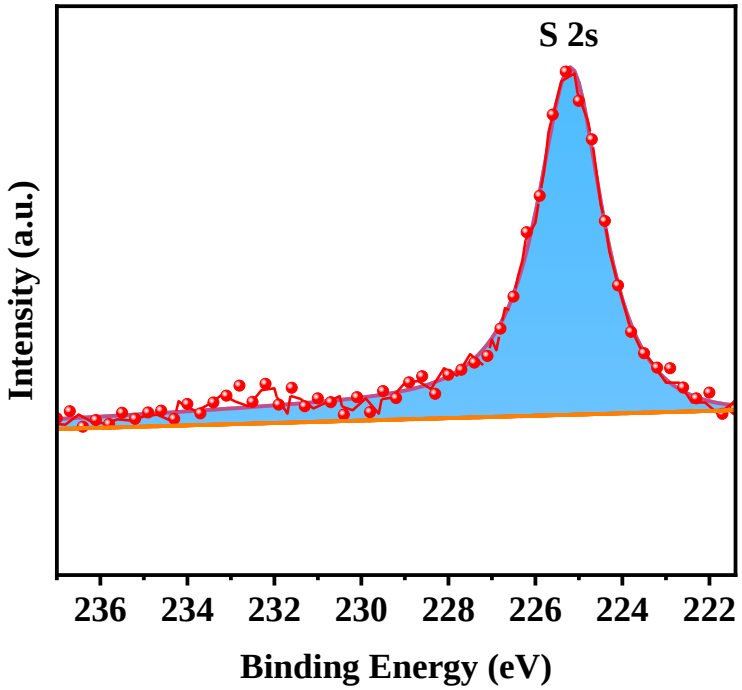

Figure S1. High-resolution S 2s XPS spectrum of Bi_2S_3 nanowires.

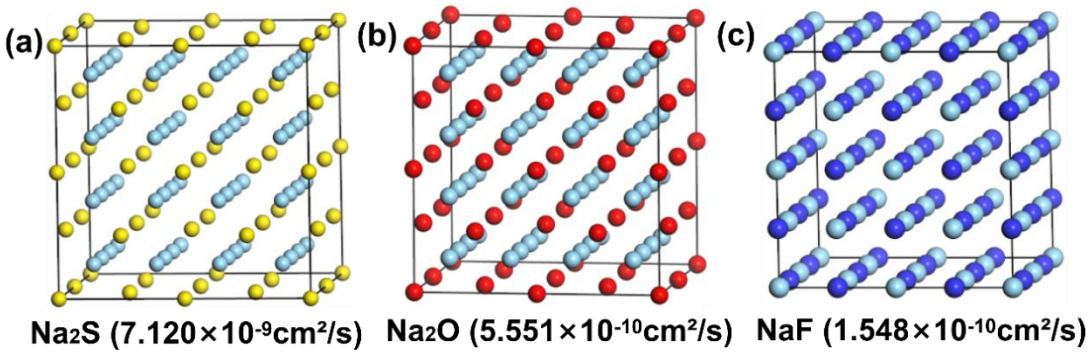

Figure S2. Supercell structures of (a) Na_2S, (b) Na_2O and (c) NaF with calculated Na diffusion coefficients.

Table S1. Calculation of Na diffusion coefficients in Na2O, NaF, and Na2S

Structure	Diffusion coefficie(cm^2/s)
Na_2O	5.551×10^{-10}
Na_2S	7.120×10^{-9}
NaF	1.548×10^{-10}

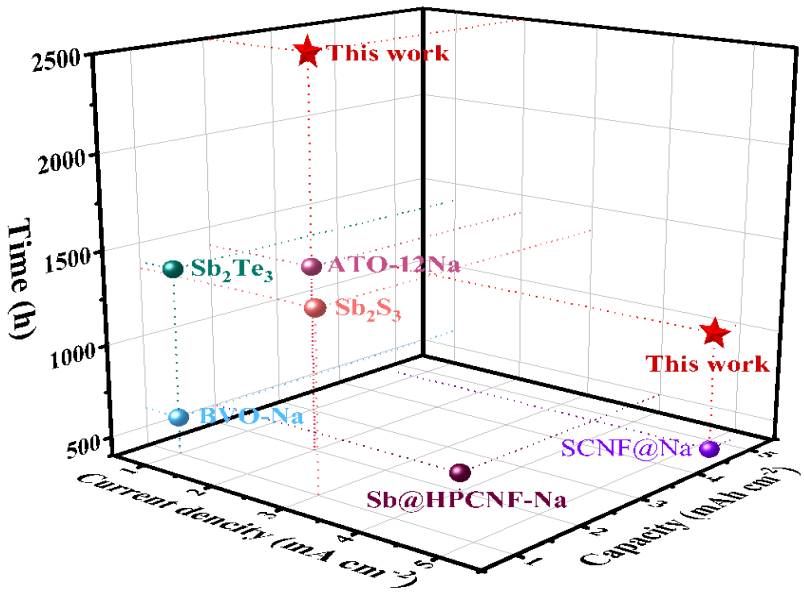

Figure S3. Comparison of the electrochemical performances between the present Na/Bi_2S_3 electrode and previously reported SMA materials in symmetric cells using ether-based electrolytes.

Table S2. The performance comparison of Na/Bi_2S_3 symmetric cells in this work and other strategies reported in the previous literature

No.	Structure	Current Density (mA cm^{-2})	Capacity (mAh cm^{-2})	Cycle	Time (h)	Ref.
1	BVO-Na	1	1	500	1000	1
2	Sb_2Te_3	1	1	700	1400	2
		3	3	800	1600	
		2	6	266	1600	
3	ATO-12Na	1	1	480	960	3
		2	2	700	1400	
		4	2	170	170	
4	Sb_2S_3	3	1	2000	1367	4
		3	3	700	1400	
		5	5	500	1000	

5	SCNF@Na	3	3	500	1000	5
		5	5	175	350	
6	Sb@HPCNF-Na	2	2	500	1000	6
		4	2	500	500	
		5	5	275	550	
7	Bi_2S_3	2	2	1250	2500	This
		3	1	1800	1200	wok
		5	5	500	1000	

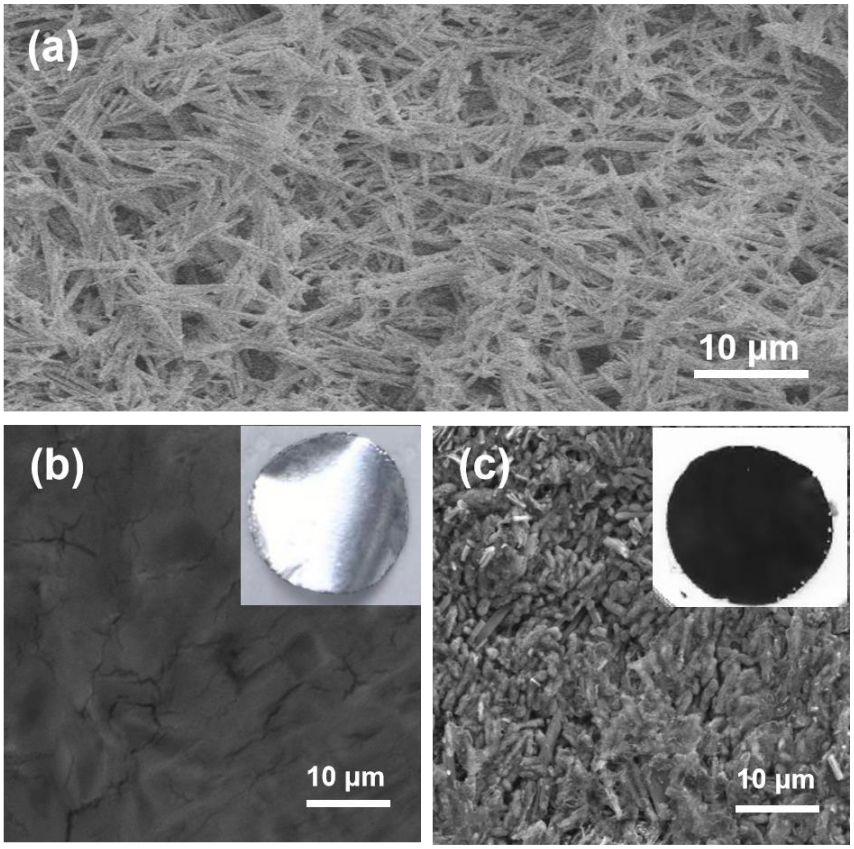

Figure S4. (a) Pristine Bi_2S_3 nanowire networks on Cu substrate before cycling. (b, c) SEM images of the Bi_2S_3@Cu substrates after (b) plating and (c) stripping at 3 mA cm^{-2} with 3 mAh cm^{-2}.

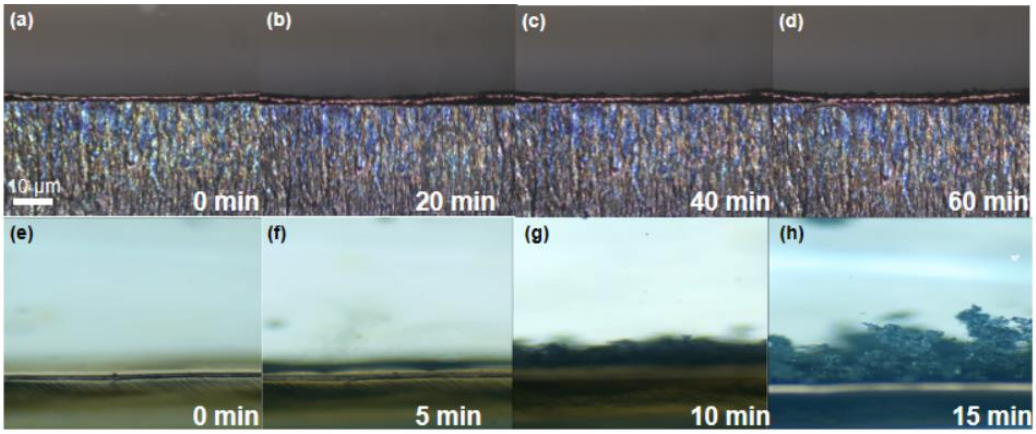

Figure S5. In-situ optical microscopy visualization of sodium plating processes at 1 mA cm^{-2}. Sequential images taken on the (a-d) Bi_2S_3@Cu and (e-h) bare Cu substrates at different plating times.

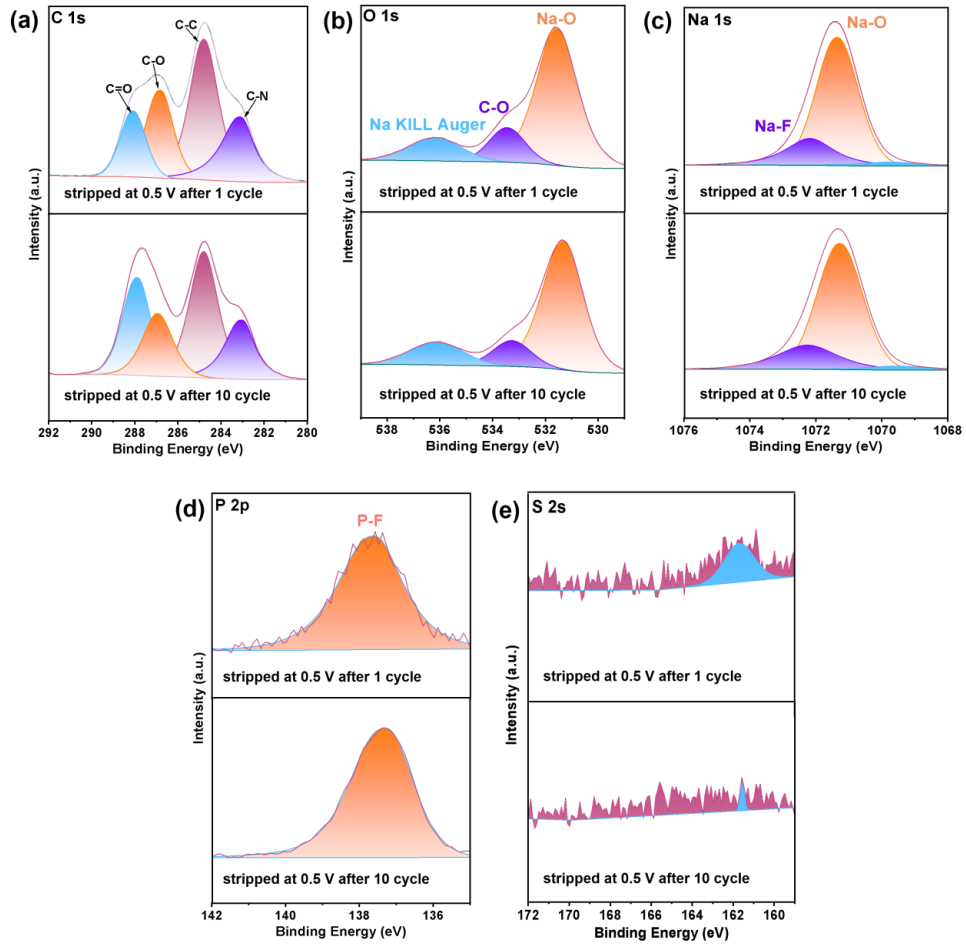

Figure S6. Ex-situ XPS spectra of the Bi_2S_3@Cu substrate after different plating/stripping cycles at 0.5 mA cm^{-2} and 3 mAh cm^{-2}.

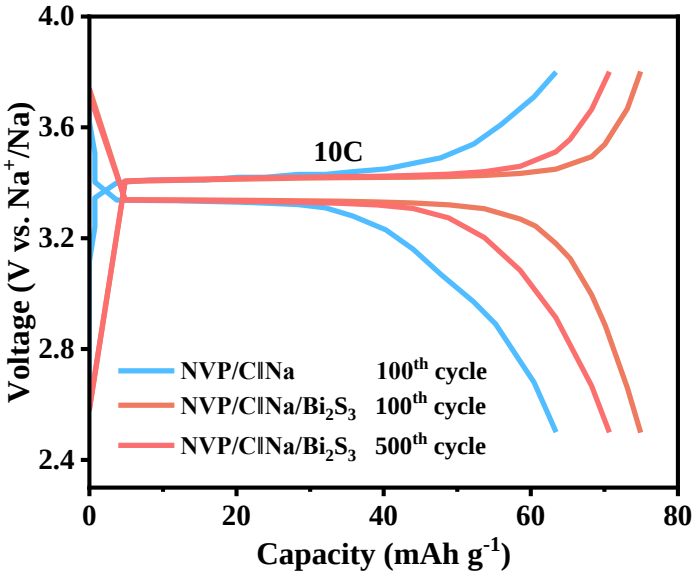

Figure S7. GCD profiles at 10C for the the NVP/C‖Na/Bi_2S_3 and NVP/C‖Na full cells.

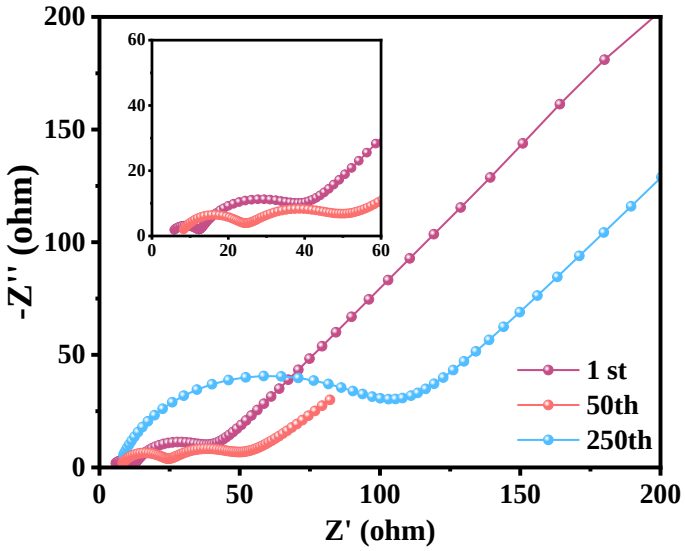

Figure S8. Nyquist plots of the NVP/C‖Na full cells after different cycles.

For the NVP/C‖Na full cell (Figure S7), the initial charge-transfer resistance (R_{ct}) is as high as 18 Ω. After only 250 cycles at 10 C, the R_{ct} increases sharply to 89 Ω. This dramatic rise is attributed to the continuous growth of an unstable, thick, and poorly conductive SEI layer caused by severe Na dendrite formation and repeated interfacial fracture/repair processes, which progressively block charge transfer across the electrode/electrolyte interface. In contrast, the Bi_2S_3@Cu full cell (Figure 6e) exhibits

an ultralow initial R_{ct} of only 5 Ω. After 100 cycles at 10 C, the R_{ct} remains as low as 13 Ω, and even after 1000 cycles it is only 24 Ω. This remarkable stability and low charge-transfer barrier directly evidence the effectiveness of the in-situ formed sodiophilic Na_3Bi/Na_2S composite interface layer, which not only promotes uniform Na nucleation and deposition but also sustains rapid Na^+ transfer kinetics over long-term cycling.

REFERENCES

(1) Yu, H. L.; Jiang, D. C.; Cheng, X. L.; Lu, P.; Li, S. K.; Zhang, H.; Jiang, Y.; Huang, F. Z. Ultrastable Sodium/Potassium Metal Anode Enabled by a Multifunctional Interphase Layer with Enhanced Ion Transport Kinetics. *Advanced Functional Materials* **2023**, *33* (52), 10. DOI: 10.1002/adfm.202307628.

(2) Chen, B. F.; Zhao, Y. S.; Yuan, B. Y.; Zhu, Y. X.; Chong, S. K. Antimony Telluride as Bifunctional Host Material for Dendrite-Free Sodium Metal Batteries. *Nano Letters* **2025**, *25* (12), 4869-4877. DOI: 10.1021/acs.nanolett.4c06650.

(3) Li, Z. P.; Miao, L. C.; Lin, G. L.; Tian, W. Y.; Yuan, S. H.; Si, Y. C.; Wang, Q. L.; Jiao, L. F. Na (100)-Textured Electrode Embedded with Sb-Doped SnO2 Nanoparticles for Dendrite-Free Sodium Metal Batteries. *Advanced Energy Materials* **2024**, *14* (47). DOI: 10.1002/aenm.202402284.

(4) Chen, R. C.; Lu, X.; He, Q. R.; Yao, M. L.; Yao, T. H.; Gao, A.; Ding, S. J.; Cheng, Y. H.; Wang, H. K. Sb2S3 Nanorod Hierarchies Enabling Homogeneous Sodium Deposition for Dendrite-Free Sodium-Metal Batteries. *Acs Applied Energy Materials* **2022**, *5* (9), 10952-10960. DOI: 10.1021/acsaem.2c01625.

(5) Mubarak, N.; Rehman, F.; Ihsan-Ul-Haq, M.; Xu, M. Y.; Li, Y.; Zhao, Y. H.; Luo, Z. T.; Huang, B. L.; Kim, J. K. Highly Sodiophilic, Defect-Rich, Lignin-Derived Skeletal Carbon Nanofiber Host for Sodium Metal Batteries. *Advanced Energy Materials* **2022**, *12* (12), 13. DOI: 10.1002/aenm.202103904.

(6) Li, Z. P.; Qin, H. Y.; Tian, W. Y.; Miao, L. C.; Cao, K. Z.; Si, Y. C.; Li, H. X.; Wang, Q. L.; Jiao, L. F. 3D Sb-Based Composite Framework with Gradient

Sodiophilicity for Ultrastable Sodium Metal Anodes. *Advanced Functional Materials* **2024**, *34* (5). DOI: 10.1002/adfm.202301554.